nature plants

LETTERS

https://doi.org/10.1038/s41477-020-00773-1

Check for updates

Calcium dynamics during trap closure visualized in transgenic Venus flytrap

Hiraku Suda[1,2], Hiroaki Mano[1,2,3], Masatsugu Toyota[4,5], Kenji Fukushima[1,2,6], Tetsuro Mimura[7], Izuo Tsutsui[8], Rainer Hedrich[6,9], Yosuke Tamada[1,2,10] and Mitsuyasu Hasebe[1,2] ✉

The leaves of the carnivorous plant Venus flytrap, *Dionaea muscipula* (Dionaea) close rapidly to capture insect prey. The closure response usually requires two successive mechanical stimuli to sensory hairs on the leaf blade within approximately 30 s (refs. [1-4]). An unknown biological system in Dionaea is thought to memorize the first stimulus and transduce the signal from the sensory hair to the leaf blade[2]. Here, we link signal memory to calcium dynamics using transgenic Dionaea expressing a Ca^{2+} sensor. Stimulation of a sensory hair caused an increase in cytosolic Ca^{2+} concentration ($[Ca^{2+}]_{cyt}$) starting in the sensory hair and spreading to the leaf blade. A second stimulus increased $[Ca^{2+}]_{cyt}$ to an even higher level, meeting a threshold that is correlated to the leaf blade closure. Because $[Ca^{2+}]_{cyt}$ gradually decreased after the first stimulus, the $[Ca^{2+}]_{cyt}$ increase induced by the second stimulus was insufficient to meet the putative threshold for movement after about 30 s. The Ca^{2+} wave triggered by mechanical stimulation moved an order of magnitude faster than that induced by wounding in petioles of *Arabidopsis thaliana*[5] and Dionaea. The capacity for rapid movement has evolved repeatedly in flowering plants. This study opens a path to investigate the role of Ca^{2+} in plant movement mechanisms and their evolution.

Plants have evolved a variety of mechanisms that 'remember' external stimuli as part of numerous processes, including acclimation to harsh environments, systemic acquired resistance to pathogens and vernalization[6]. In the short-term memory system of Dionaea (Fig. 1a), the second stimulus can be to any of the leaf's six sensory hairs (Fig. 1b), regardless of which hair received the first stimulus[2]. Previous studies showed that mechanical stimulation of a sensory hair generates action potentials that propagate to both lobes of the leaf[7,8]. Other studies have shown that leaf closure is blocked by Ca^{2+} channel inhibitors that should inhibit increase of the cytosolic Ca^{2+} concentration ($[Ca^{2+}]_{cyt}$) of leaf cells, emphasizing the importance of Ca^{2+} in the response[9–11]. On the basis of these results, the mechanism of Dionaea memory has been proposed to be as follows[10,12]: (1) $[Ca^{2+}]_{cyt}$ increases during excitation; (2) $[Ca^{2+}]_{cyt}$ or the concentration of some Ca^{2+}-activated regulatory molecules must reach a threshold for movement; (3) a single action potential is not enough to increase $[Ca^{2+}]_{cyt}$ to the threshold and at least two action potentials are necessary to trigger movement; (4) $[Ca^{2+}]_{cyt}$ decreases after the first stimulus and after 30 s does not reach the threshold even with a second stimulus. This hypothesis has not been directly tested because of the lack of a method for spatiotemporal calcium monitoring in Dionaea.

Since transformation of Dionaea has not been reported, to observe spatiotemporal cytosolic $[Ca^{2+}]$ changes in Dionaea, we set out to transform excised leaves with *Agrobacterium* carrying a construct for constitutive expression of sGFP (refs. [13–15]; pSB111U2-sGFP; Supplementary Fig. 1a). On the basis of the number of leaves expressing sGFP, etiolated leaves had a significantly higher transformation rate (97% ($n=96$)) than did non-etiolated leaves (46% ($n=91$)) (two-tail $P=4.8\times10^{-12}$ by Fisher's exact test). Furthermore, shoot regeneration rates from etiolated leaves were significantly higher under continuous dark conditions (55% ($n=60$)) than under continuous light conditions (27% ($n=60$)) (two-tail $P=0.0028$ by Fisher's exact test). From 77 excised etiolated leaves, we obtained seven transgenic plants that constitutively and ubiquitously expressed sGFP (Supplementary Fig. 2).

Using the same procedures, we next produced plants transformed with a construct for constitutive expression of the calcium sensor protein GCaMP6f, which contains a cpEGFP fluorescent moiety[14,16] (pSB111U2-GCaMP6f; Supplementary Fig. 1b). Five transgenic plants were obtained from 245 excised etiolated leaves. When non-excised leaves of GCaMP6f-transgenic Dionaea were placed on ice, cpEGFP fluorescence increased in both leaf lobes and petioles (Fig. 1c), as reported for cold-treated leaves of *Arabidopsis thaliana*[17]. Cytosolic localization of cpEGFP fluorescence was observed in a cut leaf blade (Supplementary Fig. 3).

We mechanically stimulated a sensory hair of GCaMP6f Dionaea and observed that cpEGFP fluorescence increased within 0.02 s at the base of the hair (Fig. 2a), where the sensory cells that generate action potentials are located[7]. Over time, fluorescence intensity continued to increase in the sensory hair (Fig. 2a) and fluorescence spread radially from the sensory hair to the surrounding leaf tissue (Fig. 2c,d, Extended Data Fig. 1 and Supplementary Videos 1 and 2). There are non-pigmented glands and pigmented digestive glands on the leaf blade[2]. The increase of fluorescence intensity was detected in the former glands but not in the latter. Fluorescence also propagated from one lobe of the leaf to the other (Fig. 2e,f left, Extended Data Fig. 2 and Supplementary Video 3). In the abaxial view, fluorescence was not detected in the midrib (Fig. 2f right). This suggests that fluorescence is propagated in the epidermis and/or parenchyma adaxial to the midrib but not in the midrib and tissue surrounding the midrib, both of which are connected to the petiole (Fig. 2f,g).

[1]National Institute for Basic Biology, Okazaki, Japan. [2]Department of Basic Biology, The Graduate University for Advanced Studies (SOKENDAI), Okazaki, Japan. [3]JST, PRESTO, Saitama, Japan. [4]Department of Biochemistry and Molecular Biology, Graduate School of Science and Engineering, Saitama University, Saitama, Japan. [5]Department of Botany, University of Wisconsin, Madison, WI, USA. [6]Institute for Molecular Plant Physiology and Biophysics, University of Würzburg, Würzburg, Germany. [7]Department of Biology, Graduate School of Science, Kobe University, Kobe, Japan. [8]Graduate School of Business Administration, Hitotsubashi University, Kunitachi, Japan. [9]Zoology Department, College of Science, King Saud University, Riyadh, Saudi Arabia. [10]School of Engineering, Utsunomiya University, Utsunomiya, Japan. ✉e-mail: mhasebe@nibb.ac.jp

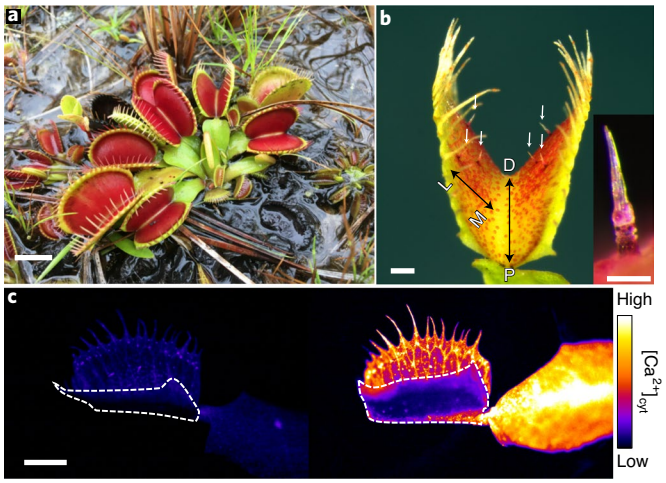

Fig. 1 | Cold stimulation induces a $[Ca^{2+}]_{cyt}$ increase in a Dionaea trap leaf. a, A Dionaea plant growing in its natural habitat, North Carolina, United States. Leaves form a rosette and the bilobed leaf blade of each leaf forms a trap. **b**, Six sensory hairs (arrows) of a Dionaea leaf, one of which is magnified in the inset. L, lateral direction; M, medial direction; D, distal direction; P, proximal direction. Similar results were obtained from three leaves of three biologically independent plants. **c**, GCaMP6f fluorescence images of a leaf blade before (left) and 2 min after (right) a cold stimulus. The abaxial side of a petiole and right half of a leaf blade (a right leaf lobe) were attached to an ice block and cpEGFP signals were detected in cells attached to the ice. The left leaf lobe (outlined by dashed line) did not touch the ice block and the cpEGFP signal was not detected. Scale bars, 1 cm in **a**; 1 mm in **b** and **c**; 100 µm in the inset of **b**.

This is consistent with the observation that fluorescence did not propagate into the petiole (Fig. 2f).

We could not localize fluorescence to specific cells because of the difficulty of observing intact cells deep within the leaf and the need to avoid wound-induced fluorescence that would be caused by physical dissection (Supplementary Fig. 3). The fluorescence signal extended laterally as far as the area where secondary leaf veins, which run perpendicularly from a primary vein in the midrib toward the leaf edges, begin to branch and merge with neighbouring veins (Fig. 2h). This was the furthest lateral spread observed on both the adaxial and abaxial sides of the leaf (Fig. 2f).

The average propagation velocity in the medial direction (53 ± 8.2 mm s^{-1} (mean ± s.e.m., $n = 8$ leaves)) was faster than that in the lateral direction (20 ± 6.8 mm s^{-1} (mean ± s.e.m., $n = 8$ leaves)). Average velocities in the proximal and distal directions were similar to that in the lateral direction (23 ± 3.2 mm s^{-1} (mean ± s.e.m., $n = 8$ leaves) and 21 ± 3.2 mm s^{-1} (mean ± s.e.m., $n = 8$ leaves), respectively) (Fig. 2d and Extended Data Fig. 3a). The velocity did not change when the fluorescence crossed a leaf vein or the midrib (Supplementary Video 3). The Ca^{2+} wave velocities resulting from stimulation of a sensory hair and those caused by wounding to the leaf blade were not distinguished (Extended Data Figs. 3c and 4, Supplementary Table 1 and Supplementary Video 4). It should be noted that similar action potentials are produced in response to mechanical stimulation and wounding[18].

Fluorescence of unstimulated sensory hairs increased when the wave front reached them (Fig. 2c and Supplementary Video 1). This is consistent with the observation that leaf closure can be induced with a second stimulus to any sensory hair, not only the one that received the first stimulus. It is noteworthy that the Ca^{2+} wave velocities resulting from stimulation of a sensory hair as well as those caused by wounding to the leaf blade are approximately 50 to 20 times faster than those caused by wounding to petioles in *A. thaliana* (1.089 mm s^{-1}) (ref. [5]) and in Dionaea (1.2 ± 0.17 mm s^{-1} (mean ± s.e.m., $n = 5$ leaves)) (Extended Data Figs. 3d and 5 and Supplementary Video 5).

We next observed Ca^{2+} dynamics following a second stimulus. The second stimulus further increased the signal intensity of the stimulated sensory hair (Fig. 2b), then propagated radially to mostly the same area as the first stimulus did and the leaf closed (Fig. 2c, Extended Data Fig. 6 and Supplementary Video 1). Average propagation velocities for the second stimulus were approximately two to three times faster than those for the first stimulus in all four directions (Fig. 2c, Extended Data Fig. 3b, Supplementary Table 1 and Supplementary Video 1), suggesting that cells with an increased $[Ca^{2+}]_{cyt}$ caused by the first stimulus are more sensitive to a second stimulus. The leaf area with increased fluorescence was indistinguishable from the area that changed tissue curvature during the leaf closure in a previous study[19].

These results and the Ca^{2+} requirement of the snap movement[9–11] are concordant with the previous proposal that $[Ca^{2+}]_{cyt}$ increases during excitation and is involved in triggering movement[10]. However, to clarify the causality between $[Ca^{2+}]_{cyt}$ and movement, future genetic studies are necessary. The anisotropic differences in propagation velocities of the $[Ca^{2+}]_{cyt}$ increase and the acceleration of propagation velocities in response to the second stimulus (Extended Data Fig. 3 and Supplementary Table 1) are qualitatively in agreement with the behaviour of leaf action potentials[8]. However, the action potentials propagate at 60–170 mm s^{-1} after the first stimulus and 250 mm s^{-1} after the second stimulus[8,20], much faster than the propagation of $[Ca^{2+}]_{cyt}$ changes (20–53 mm s^{-1} after the first stimulus, 51–102 mm s^{-1} after the second stimulus; Supplementary Table 1). Furthermore, lateral movement of the $[Ca^{2+}]_{cyt}$ wave stops once it reached the area where the secondary veins branch (Fig. 2f), while action potentials continue beyond that boundary to reach the margin of the leaf blade[8]. These results suggest that propagation of the $[Ca^{2+}]_{cyt}$ wave is not directly linked to that of the action potentials. Since different experimental setups result in variable velocities of action potentials[21], a measurement of action potentials in GCaMP6f Dionaea together with $[Ca^{2+}]_{cyt}$ changes with an intact leaf is necessary to further investigate the relationship between $[Ca^{2+}]_{cyt}$ wave and action potential, although it is not possible at this stage in Dionaea.

To investigate whether the need for two stimuli can be explained by there being a $[Ca^{2+}]_{cyt}$ threshold for movement[10], we quantitated GCaMP6f fluorescence intensity in the lateral and central areas of leaf blades (Fig. 2h) every 0.02 s after a mechanical stimulus to a sensory hair (Fig. 3a,b). We normalized fluorescence intensity at time t to the maximum intensity after the first stimulus, to yield relative intensity F_t (Fig. 3a and Extended Data Fig. 7). The first stimulus triggered an elevation in fluorescence intensity, which then gradually decreased in both areas of the leaf (Fig. 3a,b). Fluorescence increased additively in response to the second stimulus in both areas and then the leaf closed. The maximum fluorescence intensity after the second stimulus was higher than that reached after the first stimulus. Fluorescence intensities after the start of leaf movement could not be accurately measured because of the rapid movement.

Because movement is triggered by the second stimulus, we measured the residual F_t immediately before the second stimulus (F_{res}) and the maximum F_t just after the second stimulus (F_{max}) (Fig. 3a). Logistic regression analysis showed that F_{res} in both lateral and central areas are significantly correlated with leaf closure (Fig. 3c and Table 1). However, F_{max} in the lateral area, but not in the central area, are significantly correlated with leaf closure. It is possible that $[Ca^{2+}]_{cyt}$ exceeded the detection range of GCaMP6f in the central area after the second stimulus, because fluorescence intensity was higher in the central area than in the lateral area (Extended Data Fig. 7). The predicted 95% confidence intervals (CI) of putative threshold F_{res}, where leaf closure is triggered with 50% probability,

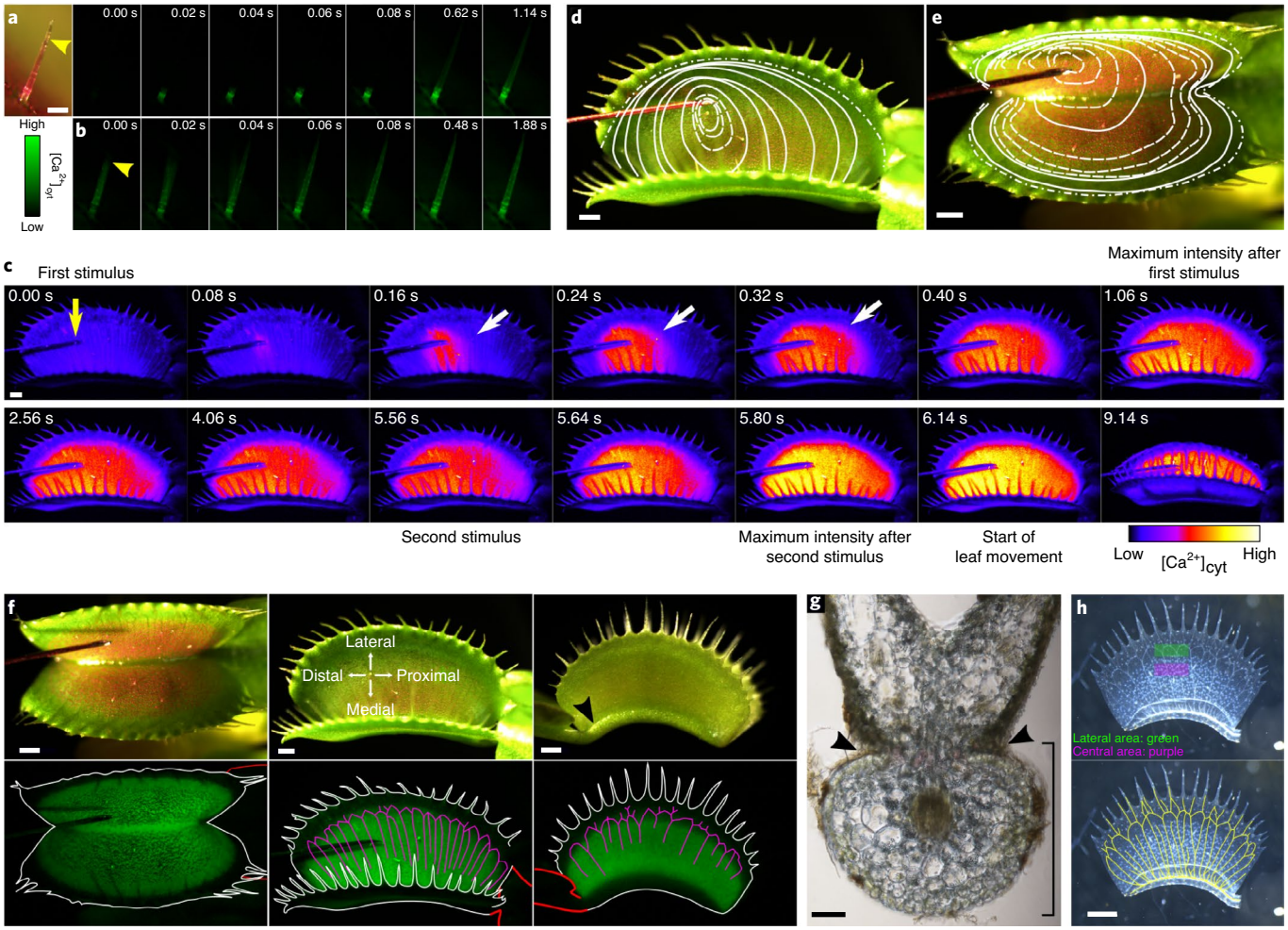

Fig. 2 | A $[Ca^{2+}]_{cyt}$ increase propagates from the sensory hair to the leaf blade after mechanical stimulation. a,**b**, Bright-field (**a**, leftmost) and fluorescence (others) images of a sensory hair stimulated by a needle at the indicated position by arrow heads. Seconds (s) from the first (**a**) or second (**b**) stimulus is indicated. Rightmost fluorescence images are the frames with the maximum intensity scored after the stimulus. Maximum intensity was measured across the whole pictured area. The second stimulus was applied 13.08 s after the first stimulus. Similar results were obtained from three leaves of two biologically independent plants. **c**, Fluorescence images of a GCaMP6f Dionaea leaf blade after a sensory hair was stimulated with a needle (yellow arrow). Frames were extracted in pseudocolour from those shown in Supplementary Video 1. Seconds (s) after the first stimulus are indicated. White arrows indicate sensory hairs with fluorescence despite not having been mechanical stimulated. The leaf closed after the second stimulus. Maximum intensity was measured across the whole pictured area. **d**,**e**, Propagation of the $[Ca^{2+}]_{cyt}$ increase following the first mechanical stimulation to a sensory hair, indicated on bright-field images of the leaf shown in **c** (**d**) and in Extended Data Fig. 2 (**e**). Boundaries of the propagated area are shown every 0.02 s (white dashed line) and 0.08 s (white solid line). The boundary of the maximum propagated area is shown by a white dash-dotted line, 1.06 s (**d**) and 0.60 s (**e**) after application of the mechanical stimulus, respectively. **f**, Bright-field (top) and fluorescence (bottom) images of the adaxial (left and middle) and abaxial (right) sides of leaves showing the frame at which the maximum intensity after the mechanical stimulation was scored. Intensity was measured across the whole pictured area. White and red lines indicate outlines of a leaf blade and petiole, respectively. Magenta lines indicate leaf veins around the lateral boundary of fluorescence. **g**, Transverse section of tissue around the midrib. Black arrow heads indicate borders between fluorescent and non-fluorescent regions in the abaxial surface. The midrib is indicated by a bracket. Similar results were obtained from three leaves of three biologically independent plants. **h**, Bright-field images of a cleared leaf blade. Lateral and central areas used in the logistic regression analysis are indicated in green and magenta in the upper image. Secondary veins are indicated in the lower image (yellow lines). Scale bars, 200 µm in **a** and **b**; 1 mm in **c**–**f** and **h**; 100 µm in **g**.

were 0.3738–0.6598 and 0.2599–0.4999 in the lateral and central areas, respectively (Table 1). The 95% CI of putative threshold F_{max} was 1.226–1.422 in the lateral area. A likelihood ratio test rejected the assumption that leaf closure does not depend on $[Ca^{2+}]_{cyt}$ (Table 1). These results indicate that there are putative $[Ca^{2+}]_{cyt}$ thresholds for immediately before and after the second stimulus that should be met for movement to occur. Since the predicted 95% CI of putative threshold F_{max} (1.226–1.422) is higher than that for F_1 (1.000), a single stimulus cannot raise $[Ca^{2+}]_{cyt}$ over the putative threshold F_{max} and a second stimulus is necessary to meet the putative threshold for movement, at least in the lateral area.

Next, we examined whether a second stimulus could raise $[Ca^{2+}]_{cyt}$ to the threshold after the memory limit time of 30 s after the first stimulus[2,3]. We measured F_t every 0.02 s after the time of F_1 in the absence of a second stimulus (Fig. 3d,e). $[Ca^{2+}]_{cyt}$ decreased with time in both lateral and central areas of the leaf and decay curves were well fit into the two-phase exponential curves with lower Akaike's Information Criterion in comparison to other simpler models (Supplementary Fig. 4). F_{res} and F_{max} in the separate experiments with the second stimulus were plotted on the same graph with showing whether the leaf closed or not at given time (Fig. 3d,e). Leaf closure depends on the time elapsed after F_1 is reached. Logistic regression analysis

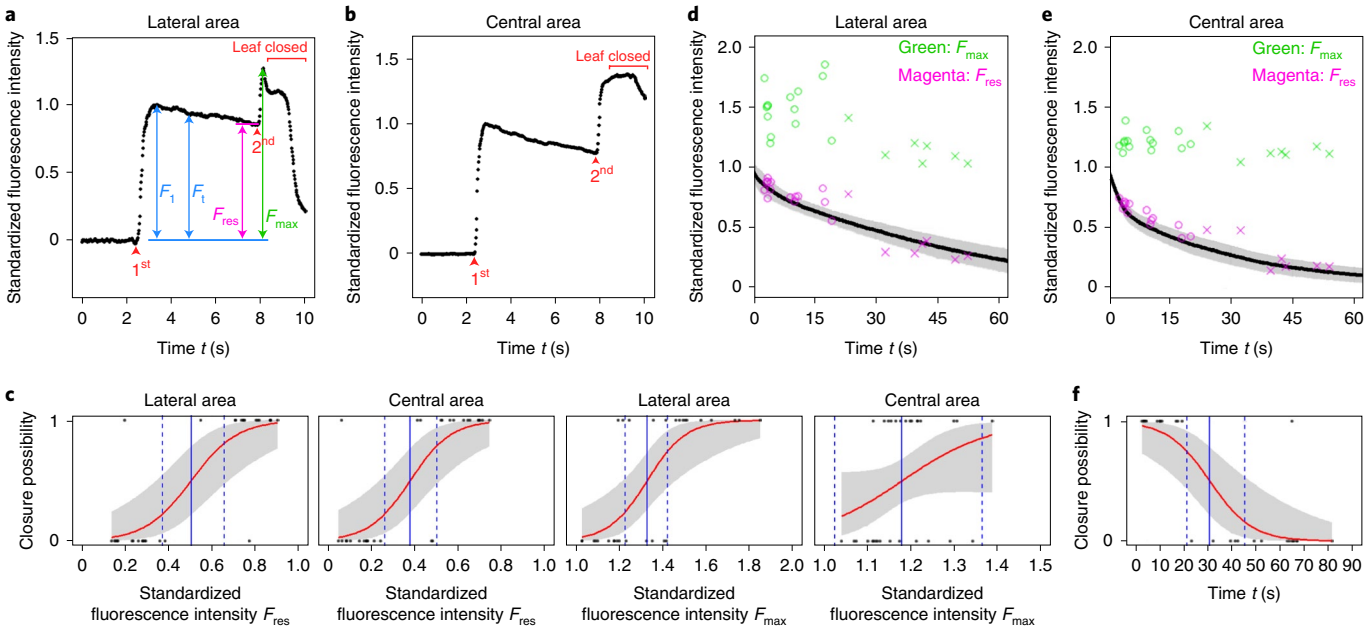

Fig. 3 | Quantitative analysis of temporal fluorescence changes after mechanical stimulation and the putative $[Ca^{2+}]_{cyt}$ threshold at which movement is triggered. a,**b**, Representative time courses of the normalized fluorescence intensity at time *t* (F_t) in the lateral (**a**) and central (**b**) areas. First and second stimuli are indicated as 1st and 2nd, respectively. The leaf closed after the second stimulus. F_1, maximum F_t after the first stimulus before the second stimulus; F_{res}, F_t immediately before the second stimulus; F_{max}, maximum F_t after the second stimulus. Plots of fluorescence intensity without normalization are shown in Extended Data Fig. 7. **c**, Regression curves in the logistic regression analyses of F_{res} at lateral areas (leftmost), F_{res} at central areas (second left), F_{max} at lateral areas (second right) and F_{max} at central areas (rightmost). Leaf states (black dots: 1, closed; 0, open), regression curve (red lines), 95% CI of the regression curve (grey regions), predicted putative thresholds of F_t to trigger closure of 50% leaves (solid blue lines) and 95% CI of the putative threshold (dashed blue lines) are shown. **d**,**e**, Decay curves of the fluorescence intensity (F_t) after F_1 is reached in the lateral (**d**) and central (**e**) area. The mean (black line) and standard deviation of the mean (grey region) are plotted every 0.02 s ($n = 6$, leaves from two biologically independent plants). F_{res} (magenta) and F_{max} (green) in **c** are plotted. Leaves were closed (circles) or not (x). **f**, Regression curves in the logistic regression analyses of duration between the first and second stimuli. Leaf states (black dots: 1, closed; 0, open), regression curve (red lines), 95% CI of the regression curve (grey regions), predicted putative thresholds of F_t to trigger closure of 50% leaves (solid blue lines) and 95% CI of the putative threshold (dashed blue lines) are shown.

Table 1 | Putative thresholds of $[Ca^{2+}]_{cyt}$ and duration with logistic regression analyses

Explanatory variable	Area	Threshold (95% CI)[a]	Odds ratio (95% CI)[b]	Maximum likelihood	Likelihood ratio test
F_{res}	Lateral	0.5058 (0.3738–0.6598)	1.165×10^4 (1.32×10^2–1.145×10^7)	2.2×10^{-4}	0.000002***
	Central	0.3756 (0.2599–0.4999)	4.114×10^4 (2.141×10^2–1.382×10^8)	9.023×10^{-5}	0.000008***
F_{max}	Lateral	1.327 (1.226–1.422)	7.627×10^4 (1.558×10^2–7.536×10^8)	8.301×10^{-6}	0.000044***
	Central	1.179 (1.026–1.364)	1.608×10^4 (0.932–3.825×10^9)	6.17×10^{-9}	0.063311
Duration	–	30.88 s (21.4–45.42)	0.8917 (0.8093–0.9446)	3.229×10^{-4}	0.000001***

[a]Value of F_{max} or F_{res} where half number of the trap leaves close. [b]Effect size calculated from the regression coefficient. [a,b]95% CI: predicted 95% confidence intervals of putative threshold. ***$P < 0.001$ ($n = 30$).

showed that the putative 50% leaf closure threshold for the duration of the F_1 signal was 30.88 s with 95% CI 21.4–45.42 s (Fig. 3f and Table 1), which concurs with previous studies[2,3]. The means of $F_{30.88}$ in the lateral and central areas were 0.4631 ± 0.07214 (mean ± s.e.m., $n = 6$ leaves) (Fig. 3d) and 0.2638 ± 0.07758 (mean ± s.e.m., $n = 6$ leaves) (Fig. 3e), respectively, which are within the ranges of 95% CIs of putative F_{res} thresholds (Table 1). These results indicate that the time course of $[Ca^{2+}]_{cyt}$ decay correlates with the duration of the signal produced by the first stimulus and that the 30-s length of memory is explained by the decay of $[Ca^{2+}]_{cyt}$.

We also investigated whether the third stimulus can increase $[Ca^{2+}]_{cyt}$ over the putative threshold F_{max} and trigger movement, when the second stimulus does not trigger movement. After the third stimulus, F_t at the lateral area reached the 95% CI of the putative threshold and the leaf closed (Extended Data Fig. 8 and Supplementary Fig. 5 and Supplementary Video 6). On the other hand, even when F_t at central area reached the 95% CI of the putative threshold, the leaf did not close (Supplementary Fig. 5 and Extended Data Fig. 8). These results are concordant with the result that F_{max} at lateral area significantly correlates to the movement but F_{max} at central area does not (Table 1).

To further investigate relationships between the putative $[Ca^{2+}]_{cyt}$ threshold and movement, two experiments were used. We found that Dionaea leaves close with no mechanical stimuli within 1 min,

when a leaf is removed from a stem at the attached position and the basal part of a petiole was immediately put in water. Even with no mechanical stimuli, the $[Ca^{2+}]_{cyt}$ signal increased two or three times and the leaf closed (Extended Data Fig. 9, Supplementary Fig. 6 and Supplementary Video 7). Before the leaf closure, $[Ca^{2+}]_{cyt}$ signals reached within the 95% CIs of the putative threshold (Extended Data Fig. 9). As the second experiment, we immersed a whole leaf in the calcium channel blocker La^{3+} solution[9,11] to reduce $[Ca^{2+}]_{cyt}$ levels. Although we do not know the reason, after 30 min of immersion with no mechanical stimuli, fluorescence intensity increased at the marginal area of the leaf blade, where Ca^{2+} waves caused by a mechanical stimulus to the sensory hair did not reach (Supplementary Fig. 7). In a whole leaf immersed in water as a control, the second mechanical stimulus raised $[Ca^{2+}]_{cyt}$ over the putative threshold to close the leaf (Extended Data Fig. 10a, Supplementary Fig. 8a and Supplementary Video 8). On the other hand, $LaCl_3$-treated leaves did not move even after the third stimulus and $[Ca^{2+}]_{cyt}$ did not reach 95% CI of the putative threshold at the lateral area (Extended Data Fig. 10b, Supplementary Fig. 8b and Supplementary Video 9). These results are concordant with the hypothesis that leaf movement is triggered when the $[Ca^{2+}]_{cyt}$ surpasses the threshold for the movement.

This study shows that (1) the first mechanical stimulus to a sensory hair increases $[Ca^{2+}]_{cyt}$ in the leaf tissue responsible for movement, (2) the elevated $[Ca^{2+}]_{cyt}$ decreases two-phase exponentially after the first stimulus, (3) the second stimulus additively increases $[Ca^{2+}]_{cyt}$, (4) $[Ca^{2+}]_{cyt}$ meets a putative threshold for movement after the second stimulus and (5) the time course of $[Ca^{2+}]_{cyt}$ decay after the first stimulus and the putative $[Ca^{2+}]_{cyt}$ threshold for movement are consistent with a memory system in Dionaea. Further studies on Dionaea leaf movement will reveal the molecular mechanisms of calcium dynamics to trigger movement especially on the relationships of $[Ca^{2+}]_{cyt}$ change to mechanostimulus, action potentials and turgor changes to trigger movement, as well as the evolution of rapid movement in plants. In addition, since the leaf area with increased $[Ca^{2+}]_{cyt}$ corresponds to the area in which the effective quantum yield of photosystem II transiently decreases after the mechanical stimulus to the sensory hair[22,23], studies on the relationships between $[Ca^{2+}]_{cyt}$ dynamics and other physiological responses will give insight into the evolution of carnivory in plants.

Methods

Plant materials and culture conditions. Seeds of Dionaea were kindly provided by J. Mundy (University of Copenhagen, Denmark)[24] and sterilized in 80% (v/v) EtOH for 1 min, 1% (w/v) benzalkonium chloride for 5 min and 1% (w/v) sodium hypochlorite for 5 min. The seeds were rinsed three times in water and were sown on the half-strength Murashige and Skoog (MS) medium containing 3% (w/v) sucrose, 1× Gamborg's vitamins, 0.1% (w/v) 2-(*N*-morpholino)ethanesulfonic acid, 0.05% (v/v) Plant Preservative Mixture (Plant Cell Technology) and 0.3% (w/v) phytagel. The seeds were incubated at 25 °C in continuous light until germination. Plants were cultured on modified cocultivation medium[15] (half-strength basal MS salts (1/2 MS; Wako) medium with 2% (w/v) sucrose, 1× Gamborg's vitamins (Sigma-Aldrich), 0.1% (w/v) 2-(*N*-morpholino)ethanesulfonic acid (Dojindo Laboratories) at pH 6.1) with 0.3% (w/v) phytagel (Sigma-Aldrich) in a tissue culture vessel (CUL-JAR300; AGC Techno Glass) under continuous light conditions at 25 °C. For transformation, Dionaea plants cultivated under continuous light conditions were moved to continuous dark conditions and cultivated for 1–6 months to collect etiolated leaves.

Transformation. To generate transgenic Dionaea constitutively expressing sGFP or GCaMP6f, the superbinary acceptor vector pSB1 and the superbinary intermediate vector pSB11 harbouring the *sGFP* or *GCaMP6f* sequence[13,16,25] were individually introduced into LBA4404 *Agrobacterium*[26]. *Agrobacterium* was cultivated on solid LB medium (Sigma-Aldrich) supplemented with 1.5% (w/v) agar (Nacalai Tesque) and 50 μg ml^{-1} (w/v) of hygromycin-B (Life Technologies) for 48 h at 30 °C. A single *Agrobacterium* colony was inoculated into 5 ml of liquid LB medium with 25 μg ml^{-1} (w/v) of hygromycin-B and precultured at 28 °C for 24 h with shaking at 180 r.p.m. Then, a portion of *Agrobacterium* was diluted to a concentration of optical density OD_{600} 0.15 with 40 ml of liquid LB medium supplemented with 25 μg ml^{-1} of hygromycin-B in a 200-ml baffled flask and further cultivated at 28 °C with shaking at 180 r.p.m. until an OD_{600} of ~0.55 was reached. After centrifugation at 5,000*g* for 10 min at 25 °C, the supernatant was removed and precipitated *Agrobacterium* cells were resuspended to OD_{600} 0.3 in the modified cocultivation medium mentioned above with 40 μg ml^{-1} of acetosyringone (Wako) after washing with the modified cocultivation medium once. Etiolated leaves were cut at the middle of the petiole, submerged in 10 ml of the *Agrobacterium* suspension and placed twice successively under a vacuum (−0.08 MPa in gauge pressure) for 10 min. The infected leaves were submerged in the modified cocultivation medium with fresh *Agrobacterium* and cultivated under continuous darkness at 25 °C for 72 h. *Agrobacterium*-infected leaves were transplanted onto the modified cocultivation medium with 0.3% (w/v) phytagel and 150 μg ml^{-1} of cefotaxime sodium salt (SANOFI) and cultivated under continuous darkness at 25 °C. The solid medium was exchanged once a week for at least a month, until transgenic shoots formed. One month after infection, the leaves were transferred to solid 1/2 MS medium plates lacking cefotaxime sodium salt. Transgenic shoots were cultivated under 8 h light/16 h darkness at 25 °C until green leaves formed and acclimated under 16 h light/8 h darkness at 22 °C in soil consisting of peat moss and perlite at a ratio of 2 to 1.

Tissue clearing. Leaves were fixed in 20% (v/v) acetic acid (Wako) dissolved in ethanol (Wako) with four 15-min rounds of decompression to −0.08 MPa in gauge pressure at room temperature and then kept overnight at 4 °C. Fixed leaves were rehydrated using a dilution series of ethanol (90%, 70%, 50%, 30% and 0%) and cleared in a solution consisting of 8 g of chloral hydrate (Wako), 1 ml of glycerol (Wako) and 2 ml of distilled water for 3 d at room temperature under continuous dark conditions.

Microscopy. Stereoscopic images and videos were taken using a SZX16 (Olympus) fluorescence microscope equipped with a SZX2-FGFP long-pass filter (Olympus) and a digital camera DP74 (Olympus). Fluorescence videos were taken using the linear mode of cellSens Standard (1.17) in a range where the fluorescence intensities of samples and brightness values of captured images are linear. All fluorescence movies were taken at 50 frames per second, with a 2-ms exposure time (Fig. 2a, b) or 15-ms exposure time (others) and 16× gain, in linear contrast mode and with 2 × 2 binning. Images were saved as a sequence of uncompressed tiff files. Blue, green and red channels were split from the original images and only green channel images were used for the analysis. All fluorescence images were pseudocoloured with green or LUT (fire lookup table) in ImageJ (1.52p). All videos were constructed from the green channel images of the original uncompressed tiff images. The time course of the two-dimensional propagation of increased fluorescence was determined by manually connecting the boundaries of fluorescent areas (Fig. 2d,e). To calculate the propagation velocity of the $[Ca^{2+}]_{cyt}$ increase, leaves and petioles were considered to be flat planes and the velocity induced by the stimulus was measured 0.04 s (Extended Data Fig. 3a,c), 0.02 s (Extended Data Fig. 3b) and 5 s (Extended Data Fig. 3d) after the stimulus. To compare the areas with increased $[Ca^{2+}]_{cyt}$ after application of the first and second stimuli, the pixel intensity distribution was classified into two distributions: pixels with large changes and pixels with small changes in intensity. Pixels with small changes were set as background and were assigned the same value in images acquired after the first and second stimulation. For quantitative analysis, two ROIs (regions of interest) were defined: the central and lateral areas, corresponding to the areas where secondary leaf veins run parallel and merge with neighbouring veins, respectively (Fig. 2h). The size of each ROI was set to at least 1,000 pixels and the average intensity per pixel in the ROI was calculated using ImageJ and data were plotted by Microsoft Excel (16.0.12325.20280) and R studio (1.2.1335). Confocal microscope images to observe localization of GCaMP6f were taken using a confocal laser microscope SP8 (Leica) with a detecting fluorescence emission of 491–534 nm for cpEGFP and 670–700 nm for autofluorescence of chloroplasts under excitation at 484 nm.

Image and regression analyses. To quantify the fluorescence intensity using multiple leaves, the fluorescence intensity was calculated at a given time t as $F_t = (f_t - f_0)/(f_1 - f_0)$, where f_t indicates fluorescence intensity at a given time t, f_0 indicates an average of f_t in 50 frames for 1 s before the first stimulus was applied and f_1 indicates the maximum f_t after the first stimulus was applied before the second stimulus was applied (Fig. 3a and Extended Data Fig. 7). For the explanatory variables of the regression analysis, the maximum F_t after the second stimulus was defined as F_{max}, the residual F_t immediately before the second stimulus was applied was defined as F_{res} and duration between times of f_1 and the second stimulus. As the dependent variables, closed and unclosed leaves after the second stimulus were scored as 1 and 0, respectively. For the likelihood ratio test, we set a null hypothesis that leaf movement is independent of F_{res} or F_{max} and an alternative hypothesis that leaf movement is dependent of F_{res} or F_{max} and tested by the parametric bootstrap test with 1,000,000 bootstrap replicates.

Vibratome sectioning. Untransformed Dionaea leaves were embedded in 5% (w/v) agar (Nacalai Tesque) in water and cut into 100-μm sections by vibratome VT1200 (Leica). Images of sections are taken using microscope BX51 (Olympus) equipped with a DS-Fi1c colour camera (Nikon).

Approximation of decay curves of $[Ca^{2+}]_{cyt}$. Using nls function in R (ref. [27]), we estimated the $[Ca^{2+}]_{cyt}$ decay curves using the two-phase exponential equation (1),

the one-phase exponential equation (2) and the linear equation (3) by nonlinear and linear least squares regressions.

$$g(t) = ae^{bt} + ce^{dt} + e \quad (1)$$

$$g(t) = ae^{bt} + c \quad (2)$$

$$g(t) = at + b \quad (3)$$

where $g(t)$ is $[Ca^{2+}]_{cyt}$, t is time and a–e are parameters.

Observation of digestive glands. Leaf lobes were cut by a razor blade, mounted to the 35-mm dish (Falcon) by double-sided tape and immersed for 0.5 h in a buffer containing 0.1 mM KCl (Wako), 10 mM $CaCl_2$ (Wako), 20 mM sorbitol (Wako) and 5 mM 2-(*N*-morpholino)ethanesulfonic acid (Dojindo Laboratories) adjusted with 2-amino-2-hydroxymethyl-1,3-propanediol (Wako) to pH 6 (ref. [28]). The most distal sensory hair was mechanically stimulated by a needle. Stereoscopic images and videos were taken using a SZX16 (Olympus) as mentioned above.

La^{3+} treatment. Leaves were cut by scissors at the proximal end of the petioles. Since $[Ca^{2+}]_{cyt}$ signals increased by wounding, the cut leaves were kept on a Petri dish for 3 min at room temperature to decrease $[Ca^{2+}]_{cyt}$ levels. Since some leaves do not respond to mechanical stimuli after the cut, the cut leaves were mechanically stimulated to confirm the elevation of $[Ca^{2+}]_{cyt}$ levels by a mechanical stimulus. The stimulated leaves with increased $[Ca^{2+}]_{cyt}$ levels were kept on a Petri dish for 3 min to decrease the $[Ca^{2+}]_{cyt}$ levels, then placed in the 35-mm dish (Falcon) and immersed in 8 ml of water or 20 mM $LaCl_3$ (Wako) solution. A 0.1% (v/v) Silwet-L77 (BMS) solution was added to diminish the surface tension that stimulates trigger hairs to close leaves. After 30 min of immersion, the liquid was removed. The treated leaves were kept without touching for 3 min and then the sensory hair was mechanically stimulated. Stereoscopic images and videos were taken using a SZX16 (Olympus) as mentioned above.

Reporting Summary. Further information on research design is available in the Nature Research Reporting Summary linked to this article.

Data availability

The data that support the findings of this study are available from the corresponding author upon reasonable request. Sequence data for genes and plasmids can be found in GenBank under the following accession numbers: sGFP (ABL09837), pSB1 (AB027255) and pSB11 (AB027256). Sequence of GCaMP6f can be found in Addgene data libraries as catalogue no. 40755. Source data are provided with this paper.

Received: 16 February 2020; Accepted: 24 August 2020;
Published online: 05 October 2020

References

1. Macfarlane, J. M. Contributions to the history of *Dionaea muscipula* Ellis. *Contr. Bot. Lab. Univ. Pennsylvania* **1**, 7–44 (1892).
2. Juniper, B. B. E., Robins, R. J. & Joel, D. M. *The Carnivorous Plants* (Academic Press, 1989).
3. Brown, W. H. & Sharp, L. W. The closing response in Dionaea. *Bot. Gaz.* **49**, 290–302 (1910).
4. Burri, J. T. et al. A single touch can provide sufficient mechanical stimulation to trigger Venus flytrap closure. *PLoS Biol.* **18**, e3000740 (2020).
5. Toyota, M. et al. Glutamate triggers long-distance, calcium-based plant defense signaling. *Science* **361**, 1112–1115 (2018).
6. Taiz, L., Zeiger, E., Møller, I. M. & Murphy, A. *Plant Physiology and Development* 6th edn (Oxford Univ. Press, 2018).
7. Benolken, R. M. & Jacobson, S. L. Response properties of a sensory hair excised from Venus's flytrap. *J. Gen. Physiol.* **56**, 64–82 (1970).
8. Sibaoka, T. Action potentials in plant organs. *Symp. Soc. Exp. Biol.* **20**, 49–73 (1966).
9. Hodick, D. & Sievers, A. On the mechanism of trap closure of Venus flytrap (*Dionaea muscipula* Ellis). *Planta* **179**, 32–42 (1989).
10. Hodick, D. & Sievers, A. The action potential of *Dionaea muscipula* Ellis. *Planta* **174**, 8–18 (1988).
11. Fagerberg, W. R. & Allain, D. A quantitative study of tissue dynamics during closure in the traps of Venus's flytrap *Dionaea muscipula* Ellis. *Am. J. Bot.* **78**, 647–657 (1991).
12. Hedrich, R. & Neher, E. Venus flytrap: how an excitable, carnivorous plant works. *Trends Plant Sci.* **23**, 220–234 (2018).
13. Chiu, W. et al. Engineered GFP as a vital reporter in plants. *Curr. Biol.* **6**, 325–330 (1996).
14. Maekawa, T. et al. Polyubiquitin promoter-based binary vectors for overexpression and gene silencing in *Lotus japonicus*. *Mol. Plant Microbe Interact.* **21**, 375–382 (2008).
15. Mano, H., Fujii, T., Sumikawa, N., Hiwatashi, Y. & Hasebe, M. Development of an *Agrobacterium*-mediated stable transformation method for the sensitive plant *Mimosa pudica*. *PLoS ONE* **9**, e88611 (2014).
16. Chen, T.-W. et al. Ultrasensitive fluorescent proteins for imaging neuronal activity. *Nature* **499**, 295–300 (2013).
17. Knight, H. & Knight, M. R. Imaging spatial and cellular characteristics of low temperature calcium signature after cold acclimation in *Arabidopsis*. *J. Exp. Bot.* **51**, 1679–1686 (2000).
18. Pavlovič, A., Jakšová, J. & Novák, O. Triggering a false alarm: wounding mimics prey capture in the carnivorous Venus flytrap (*Dionaea muscipula*). *New Phytol.* **216**, 927–938 (2017).
19. Forterre, Y., Skotheim, J. M., Dumais, J. & Mahadevan, L. How the Venus flytrap snaps. *Nature* **433**, 421–425 (2005).
20. Sibaoka, T. in *Plant Growth Substances* (Ed. Skoog, F.) 462–469 (Springer, 1980).
21. Volkov, A. G. Signaling in electrical networks of the Venus flytrap (*Dionaea muscipula* Ellis). *Bioelectrochemistry* **125**, 25–32 (2019).
22. Pavlovič, A., Demko, V. & Hudák, J. Trap closure and prey retention in Venus flytrap (*Dionaea muscipula*) temporarily reduces photosynthesis and stimulates respiration. *Ann. Bot.* **105**, 37–44 (2010).
23. Pavlovič, A., Slovaková, L., Pandolfi, C. & Mancuso, S. On the mechanism underlying photosynthetic limitation upon trigger hair irritation in the carnivorous plant Venus flytrap (*Dionaea muscipula* Ellis). *J. Exp. Bot.* **62**, 1991–2000 (2011).
24. Jensen, M. K. et al. Transcriptome and genome size analysis of the Venus flytrap. *PLoS ONE* **10**, e0123887 (2015).
25. Komari, T. et al. in *Agrobacterium Protocols* (ed. Wang, K.) 15–42 (Humana Press, 2015).
26. Hellens, R., Mullineaux, P. & Klee, H. Technical focus: a guide to *Agrobacterium* binary Ti vectors. *Trends Plant Sci.* **5**, 446–451 (2000).
27. Milliken, G. A., Bates, D. M. & Watts, D. G. Nonlinear regression analysis and its applications. *Technometrics* **32**, 219 (1990).
28. Escalante-Perez, M. et al. A special pair of phytohormones controls excitability, slow closure, and external stomach formation in the Venus flytrap. *Proc. Natl Acad. Sci. USA* **108**, 15492–15497 (2011).

Acknowledgements

We thank the Model Plant Research Facility of National Institute for Basic Biology for plant cultivation, the Japan Tobacco Plant Innovation Center for providing pSB11 and LBA4404 harbouring pSB1, National BioResource Project for supplying *Lotus japonicus POLYUBIQUITIN* promoter through Frontier Science Research Center of the University of Miyazaki, T. Murata for instructions of microscopy analyses, H. Narukawa for instructions of vibratome sections and Y. Matsuzaki for technical assistance. This work was supported by the JSPS KAKENHI (grant nos. 17J08569 to H.S., 17H05007 and 18H05491 to M.T., 18H04790 to Y.T. and 16K14761 and 17H06390 to M.H.) and DFG-funded Reinhart Koselleck project (HE 1640/42-1 to R.H.).

Author contributions

H.S., H.M., M.T., Y.T. and M.H. conceived and designed the research. K.F. established the aseptic culture. M.T. provided the GCaMP6f vector. H.S. and H.M. performed the experiments with advice from M.T., Y.T. and M.H. I.T. and T.M. suggested the experimental design. R.H. provided electrophysiological information on unpublished data. H.S. prepared the figures. H.S., Y.T. and M.H. wrote the manuscript with contributions from all authors.

Competing interests

The authors declare no competing interests.

Additional information

Extended data is available for this paper at https://doi.org/10.1038/s41477-020-00773-1.

Supplementary information is available for this paper at https://doi.org/10.1038/s41477-020-00773-1.

Correspondence and requests for materials should be addressed to M.H.

Peer review information *Nature Plants* thanks Edward E. Farmer, Andrej Pavlovic and the other, anonymous, reviewer(s) for their contribution to the peer review of this work.

Reprints and permissions information is available at www.nature.com/reprints.

Publisher's note Springer Nature remains neutral with regard to jurisdictional claims in published maps and institutional affiliations.

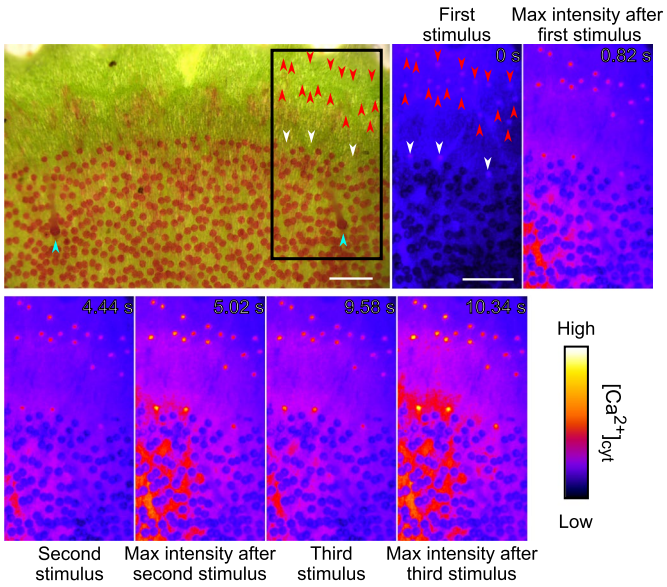

Extended Data Fig. 1 | GCaMP6f signals in glands by a series of mechanical stimuli. A bright-field image (upper leftmost) and fluorescence images (others) at the leaf blade. A pictured area of the fluorescence images corresponds to the square area at the proximal side of a leaf blade in the bright-field image. Sensory hairs are indicated by light blue arrow heads. The most distal sensory hair (left blue arrow-head) was stimulated by a needle. Pseudocolour images were extracted from those shown in Supplementary Video 2. Seconds (s) after the first stimulus are indicated. Non-pigmented glands are indicated by white arrows. We could not detect the increase of GCaMP6f signals in pigmented digestive glands by any of the three stimuli, although a previous study[28] with FURA-2 calcium indicator showed that the increase of FURA-2 signal was not detected by the first and second mechanical stimuli but was by the third stimulus. Scale bar, 1 mm.

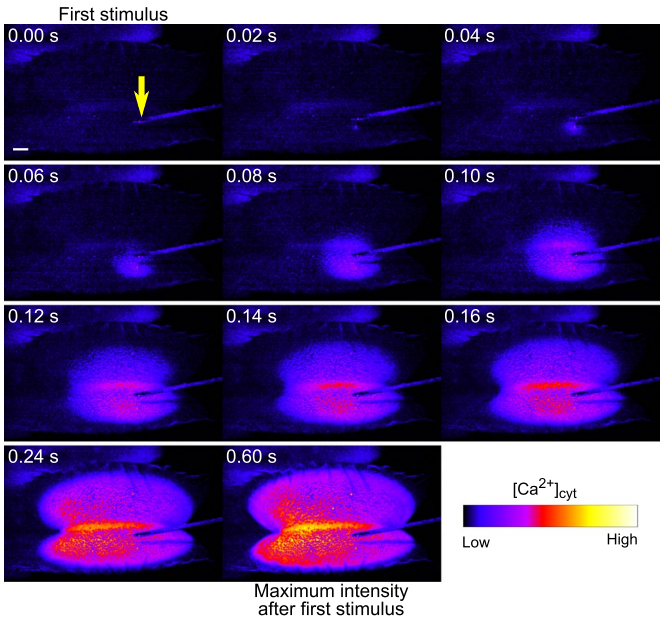

Extended Data Fig. 2 | The $[Ca^{2+}]_{cyt}$ increase induced by a mechanical stimulation propagates from the one lobe of a blade to the other. Fluorescence images of a GCaMP6f Dionaea leaf, after a sensory hair was subjected to the first mechanical stimulus with a needle (yellow arrow). Frames are extracted in pseudocolour from those shown in Supplementary Video 3. Seconds (s) after the first stimulus is indicated. Maximum intensity was measured at the whole pictured area. Scale bar, 1 mm.

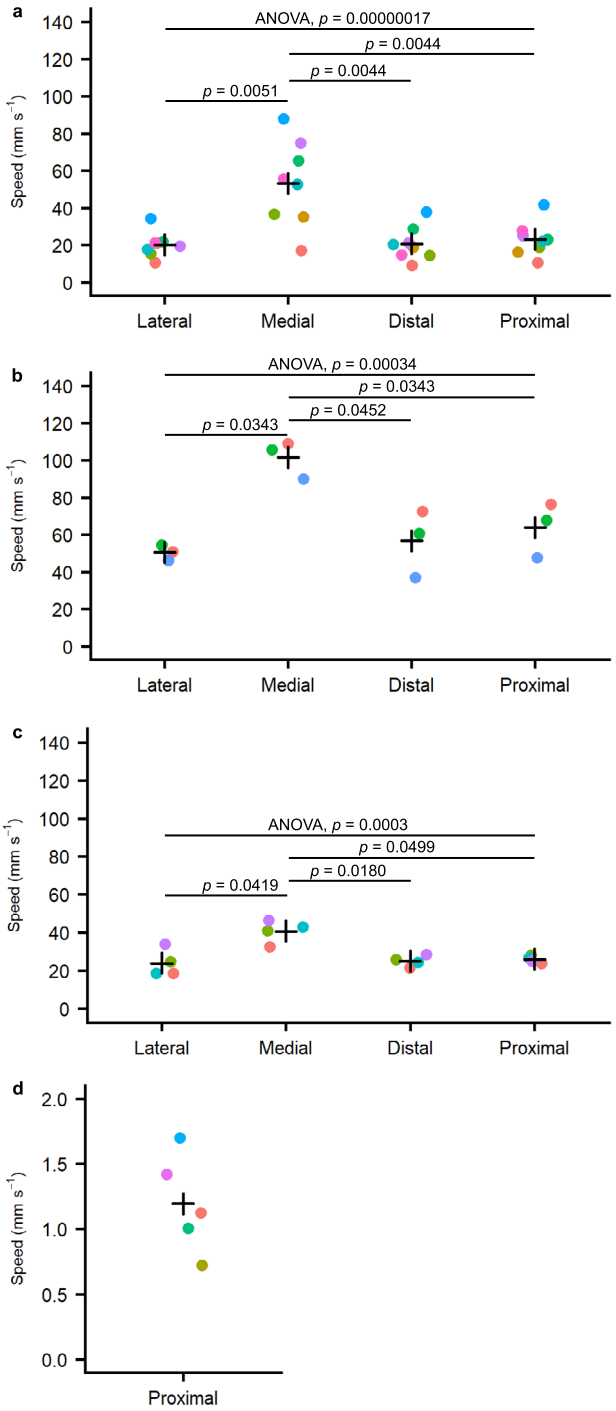

Extended Data Fig. 3 | Propagation velocity of the $[Ca^{2+}]_{cyt}$ increase. a–c, Propagation velocity of the $[Ca^{2+}]_{cyt}$ increase from a stimulated sensory hair (**a** and **b**) or from a wounded tissue (**c**). Fluorescence were measured after the first stimulus (**a**) ($n = 8$, leaves from two biologically independent plants), the second stimulus (**b**) ($n = 3$, leaves from two biologically independent plants), and the wounding stimulus by needle at the central area (**c**) ($n = 4$, leaves from two biologically independent plants) were applied. The most distal sensory hairs were mechanically stimulated after 5.18, 5.52 and 5.54 s from the first stimuli. Mean values are indicated by reticles. Velocities were measured in four directions from the stimulated site (Figs. 1b and 2f top middle). Two-way analysis of variance without replication with Holm's sequentially rejective Bonferroni procedure was used to calculate two-tail *p*-values. **d**, Propagation velocity of $[Ca^{2+}]_{cyt}$ increase by wounding ($n = 5$, leaves from two biologically independent plants). The midrib was cut at the proximal end of the leaf blade by scissors. The cut position corresponds to that in the previous study in *A. thaliana*[5]. Mean values are indicated by reticles. Velocities were measured in the proximal direction from the stimulated site (Extended Data Fig. 5).

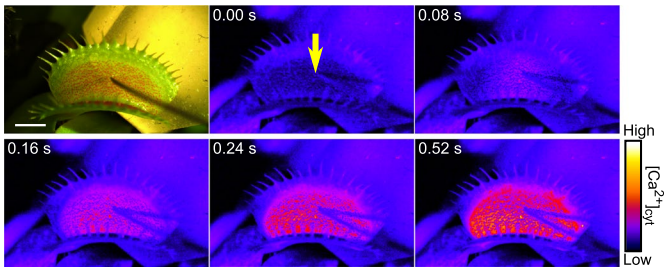

Extended Data Fig. 4 | The $[Ca^{2+}]_{cyt}$ increase induced by a wounding stimulus to the leaf blade. Bright-field image (upper leftmost) and fluorescence images (others) of a GcaMP6f Dionaea leaf wounded by a needle (yellow arrow). Frames were extracted with pseudocolour from those shown in Supplementary Video 4. Seconds (s) after the wounding stimulus is indicated. Scale bar, 2 mm.

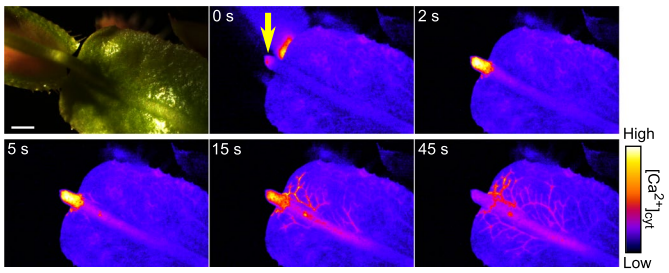

Extended Data Fig. 5 | $[Ca^{2+}]_{cyt}$ increase induced by a wounding stimulus to the midrib propagates along the midrib. Bright-field image (upper leftmost) and fluorescence images (others) of a GCaMP6f Dionaea leaf wounded by cutting with scissors (yellow arrow) the midrib at the proximal end of the leaf blade. Frames were extracted with pseudocolour from those shown in Supplementary Video 5. Seconds (s) after the wounding stimulus is indicated. Scale bar, 2 mm.

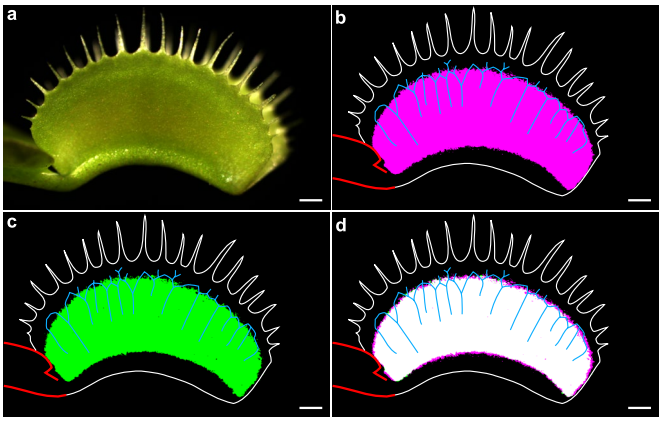

Extended Data Fig. 6 | Leaf areas exhibiting a $[Ca^{2+}]_{cyt}$ increase following the first and second stimulation overlapped. Bright-field image (**a**) and the cpEGFP fluorescence changed area at the maximum intensity frame after application of the first (**b**) and second (**c**) stimulus. Merged image of (**b**) and (**c**) is shown in (**d**). Maximum intensity was measured across the whole pictured area. White and red lines mark the boundary of the leaf blade and petiole, respectively. Blue lines indicate leaf veins around the lateral boundary of fluorescence. The second stimulus was applied 12.06 s after the first stimulus. Scale bar, 1 mm.

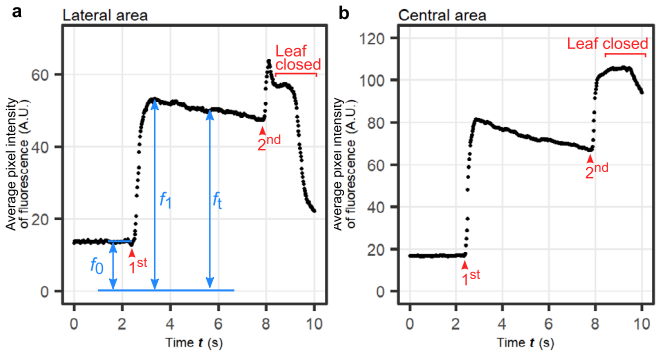

Extended Data Fig. 7 | Procedure for the normalization of fluorescence intensity. a–b, Representative time courses of the average pixel intensities of fluorescence in the lateral (**a**) and central (**b**) areas without normalization. First and second stimuli are indicated as "1st" and "2nd", respectively. After the second stimulus, the leaf closed. The normalized fluorescence intensity F_t was calculated as $(f_t-f_0) / (f_1-f_0)$, where f_t, averaged pixel intensity of fluorescence at a given time "t"; f_0, averaged f_t of 50 frames 1 s before the first stimulus; f_1, maximum f_t after the first stimulus before the second stimulus.

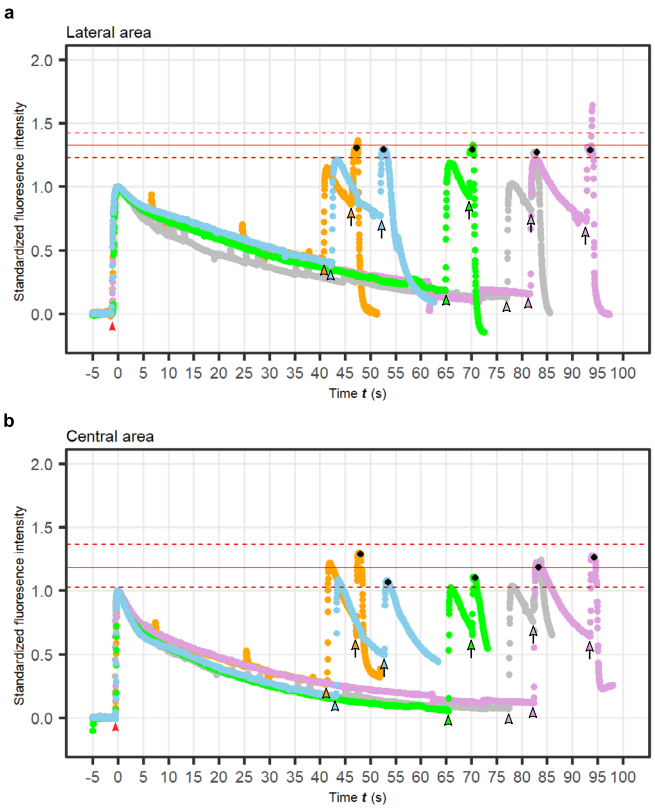

Extended Data Fig. 8 | Temporal fluorescence changes of GCaMP6f Dionaea leaves that did not close by the first and the second mechanical stimuli but closed by the third stimulus. a–b, Representative time courses of the normalized fluorescence intensity at time t [F_t] in the lateral (**a**) and the central (**b**) areas ($n = 5$, leaves from two biologically independent plants). Time at the max intensity after the first mechanical stimulus (red arrow-head) is set as 0 seconds for each experiment. The second and the third stimuli are indicated by arrow heads and arrows, respectively. The colour of arrow heads in the second and the third stimuli correspond to that of the plots. Time points when leaf movement started are indicated by black dots. Putative thresholds for the movement (red lines) and 95% CIs (red dotted lines) are taken from Table 1.

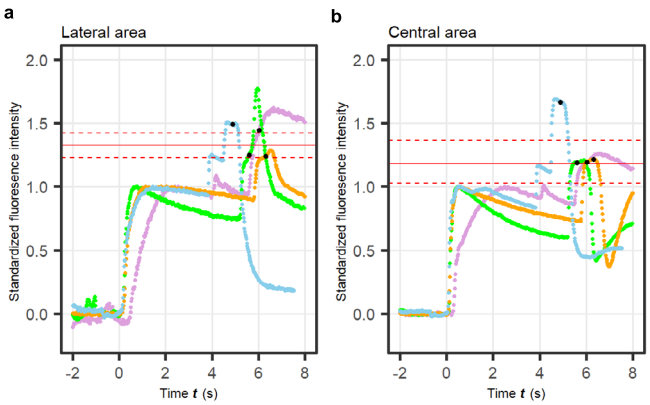

Extended Data Fig. 9 | Temporal fluorescence changes with no mechanical stimuli in a GCaMP6f Dionaea leaf whose petiole base is put in water. **a**, **b**, Representative time courses of the normalized fluorescence intensity at time t [F_t] in the lateral (**a**) and central (**b**) areas of a leaf whose petiole base was put in water ($n = 4$, leaves from two biologically independent plants). Time when fluorescence intensity started to increase without a stimulus is indicated as 0 seconds. Even though leaves were not mechanically stimulated, two or three successive increases of signals were detected. Time points when leaf movement started are indicated by black dots. Putative thresholds for the movement (red lines) and their 95% CIs (red dotted lines) are taken from Table 1.

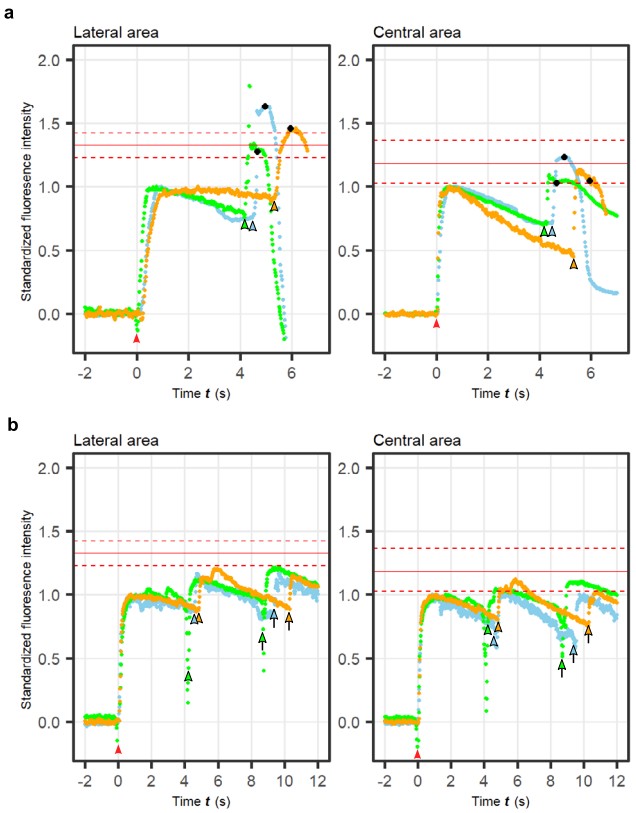

Extended Data Fig. 10 | Temporal fluorescence changes after mechanical stimulation of GCaMP6f Dionaea leaves immersed in the calcium channel blocker $LaCl_3$ solution. a–b, Representative time courses of the normalized fluorescence intensity at time t [F_t] in the lateral (left) and the central (right) areas 30 minutes after immersion in water (**a**) ($n = 3$, leaves from two biologically independent plants) or 20 mM $LaCl_3$ solution (**b**) ($n = 3$, leaves from two biologically independent plants). Time at the first mechanical stimulus (red arrow-head) is set as 0 seconds. The second and the third stimuli are indicated by arrow heads and arrows, respectively. The colour of arrow heads in the second and the third stimuli correspond to that of the plots. Time points when leaf movement started are indicated by black dots. Putative thresholds for the movement (red lines) and their 95% CIs (red dotted lines) are taken from Table 1.

nature research

Corresponding author(s): Mitsuyasu Hasebe

Last updated by author(s): Aug 15, 2020

Reporting Summary

Nature Research wishes to improve the reproducibility of the work that we publish. This form provides structure for consistency and transparency in reporting. For further information on Nature Research policies, see Authors & Referees and the Editorial Policy Checklist.

Statistics

For all statistical analyses, confirm that the following items are present in the figure legend, table legend, main text, or Methods section.

n/a	Confirmed
☐	☒ The exact sample size (*n*) for each experimental group/condition, given as a discrete number and unit of measurement
☐	☒ A statement on whether measurements were taken from distinct samples or whether the same sample was measured repeatedly
☐	☒ The statistical test(s) used AND whether they are one- or two-sided *Only common tests should be described solely by name; describe more complex techniques in the Methods section.*
☐	☒ A description of all covariates tested
☐	☒ A description of any assumptions or corrections, such as tests of normality and adjustment for multiple comparisons
☐	☒ A full description of the statistical parameters including central tendency (e.g. means) or other basic estimates (e.g. regression coefficient) AND variation (e.g. standard deviation) or associated estimates of uncertainty (e.g. confidence intervals)
☐	☒ For null hypothesis testing, the test statistic (e.g. *F*, *t*, *r*) with confidence intervals, effect sizes, degrees of freedom and *P* value noted *Give P values as exact values whenever suitable.*
☒	☐ For Bayesian analysis, information on the choice of priors and Markov chain Monte Carlo settings
☒	☐ For hierarchical and complex designs, identification of the appropriate level for tests and full reporting of outcomes
☒	☐ Estimates of effect sizes (e.g. Cohen's *d*, Pearson's *r*), indicating how they were calculated

Our web collection on statistics for biologists contains articles on many of the points above.

Software and code

Policy information about availability of computer code

Data collection	We did not use any softwares for data collection.
Data analysis	Microscopy: Fiji (ImageJ 1.52p; Java 1.8.0_172 [64-bit], https://fiji.sc/), cellSens Standard (version 1.17). Statics analysis: Rstudio version 1.2.1335, Microsoft Excel version 16.0.12325.20280.

For manuscripts utilizing custom algorithms or software that are central to the research but not yet described in published literature, software must be made available to editors/reviewers. We strongly encourage code deposition in a community repository (e.g. GitHub). See the Nature Research guidelines for submitting code & software for further information.

Data

Policy information about availability of data

All manuscripts must include a data availability statement. This statement should provide the following information, where applicable:

- Accession codes, unique identifiers, or web links for publicly available datasets
- A list of figures that have associated raw data
- A description of any restrictions on data availability

The data that Support the findings of this study are available from the corresponding author upon reasonable request. Sequence data for genes and plasmids can be found in GenBank under the following accession numbers: sGFP (ABL09837), pSB1 (AB027255) and pSB11 (AB027256). Sequence of GCaMP6f can be found in Addgene data libraries as catalog number #40755.

Field-specific reporting

Please select the one below that is the best fit for your research. If you are not sure, read the appropriate sections before making your selection.

☒ Life sciences ☐ Behavioural & social sciences ☐ Ecological, evolutionary & environmental sciences

For a reference copy of the document with all sections, see nature.com/documents/nr-reporting-summary-flat.pdf

Life sciences study design

All studies must disclose on these points even when the disclosure is negative.

Sample size	No sample-size calculation was performed. We conducted all experiments with maximum available sample size (n ≥ 3) in the same conditions including culturing, sampling, and observation. All of the sample sizes (n) were written on the manuscript.
Data exclusions	For the logistic regression analysis, we used non-moved leaves and completely closed leaves after second stimulus. We excluded incompletely closed leaves after second stimulus to exclude the leaves which did not close because of their immaturation.
Replication	We conducted all experiments with more than three biological replicates in two independent mutant lines. All replication experiments were concordant.
Randomization	We randomly sampled in all experiments.
Blinding	We were aware of sample allocation but data collection and analysis methods were not changed between sample groups.

Reporting for specific materials, systems and methods

We require information from authors about some types of materials, experimental systems and methods used in many studies. Here, indicate whether each material, system or method listed is relevant to your study. If you are not sure if a list item applies to your research, read the appropriate section before selecting a response.

Materials & experimental systems

n/a	Involved in the study
☒	☐ Antibodies
☒	☐ Eukaryotic cell lines
☒	☐ Palaeontology
☒	☐ Animals and other organisms
☒	☐ Human research participants
☒	☐ Clinical data

Methods

n/a	Involved in the study
☒	☐ ChIP-seq
☒	☐ Flow cytometry
☒	☐ MRI-based neuroimaging